PB88-251657

Compensating for Sink Effects in Emissions Test Chambers by Mathematical Modeling

Arkansas Univ., Fayetteville

Prepared for

Environmental Protection Agency
Research Triangle Park, NC

1988

U.S. Department of Commerce
National Technical Information Service
NTIS

TECHNICAL REPORT DATA
(Please read Instructions on the reverse before completing)

1. REPORT NO. EPA/600/J-88/112	2.
3. RE PB88-251657	
4. TITLE AND SUBTITLE Compensating for Sink Effects in Emissions Test Chambers by Mathematical Modeling (Journal Version)	5. REPORT DATE 1988
	6. PERFORMING ORGANIZATION CODE
7. AUTHOR(S) James E. Dunn (University of Arkansas) and Bruce A. Tichenor (EPA/AEERL)	8. PERFORMING ORGANIZATION REPORT NO.
9. PERFORMING ORGANIZATION NAME AND ADDRESS University of Arkansas Department of Mathematical Sciences Fayetteville, Arkansas 72701	10. PROGRAM ELEMENT NO.
	11. CONTRACT/GRANT NO. CR812305
12. SPONSORING AGENCY NAME AND ADDRESS EPA, Office of Research and Development Air and Energy Engineering Research Laboratory Research Triangle Park, NC 27711	13. TYPE OF REPORT AND PERIOD COVERED Published Paper; 6/86 - 2/87
	14. SPONSORING AGENCY CODE EPA/600/13

15. SUPPLEMENTARY NOTES AEERL project officer is Bruce A. Tichenor, Mail Drop 54, 919/541-2991. REF: Atmospheric Environment, 22(5):885-894, June 1988

16. ABSTRACT The paper presents mechanistic mathematical models that account for two phenomena: (1) interior surfaces of a state-of-the-art emissions test chamber acting as a transient sink for organic emissions; and (2) the effect of increasing chamber concentration on the emission rate of the source. A key point is that the effect of the chamber sink can be adjusted out simply by first fitting the appropriate model, then setting to zero the rate constant which governs sink adsorption/absorption. As a consequence of this mathematical development, a source emission rate as a function of time and a steady state emission rate factor are given precise definitions. Applications involve modeling 1,4 dichlorobenzene emission from moth crystal, and mixed emissions from latex caulk. In the first case, at a low air exchange rate and low humidity, the repressive effect of increasing vapor pressure tends to overshadow the sink effect. Increased humidity tends to offset the increase in emission rate which otherwise would occur with increased air exchange. Temperature is the principal determinant of the steady state emission rate. For the latex caulk, the effect of a sink is to retard the apparent emission rate but lengthen the period of emissions.

17. KEY WORDS AND DOCUMENT ANALYSIS

a. DESCRIPTORS		b. IDENTIFIERS/OPEN ENDED TERMS	c. COSATI Field/Group	
Pollution	Air	Pollution Control	13B	14A
Mathematical Models	Sorption	Stationary Sources		07D
Walls	Insecticides	Wall Effects	12A	06F
Test Chambers	Latex	Indoor Air Quality	13M	11J
Emission	Caulking	Moth Crystal	14B	13J
			14G	

18. DISTRIBUTION STATEMENT Release to Public	19. SECURITY CLASS (This Report) Unclassified	21. NO. OF PAGES 12
	20. SECURITY CLASS (This page) Unclassified	22. PRICE PC A02/MF A01 6.95

EPA Form 2220-1 (9-73)

REPRODUCED BY
NATIONAL TECHNICAL
INFORMATION SERVICE
U.S. DEPARTMENT OF COMMERCE
SPRINGFIELD, VA. 22161

EPA/600/J-88/112
JOURNAL ARTICLE

Atmospheric Environment Vol. 22, No. 5, pp. 883–894, 1988.
Printed in Great Britain.

0004–6981/88 $3.00 + 0.00
Pergamon Press plc

COMPENSATING FOR SINK EFFECTS IN EMISSIONS TEST CHAMBERS BY MATHEMATICAL MODELING

JAMES E. DUNN
University of Arkansas, Department of Mathematical Sciences, Fayetteville, AR 72701, U.S.A.

and

BRUCE A. TICHENOR
U.S. Environmental Protection Agency, Air and Energy Engineering Research Laboratory, Research Triangle Park, NC 27711, U.S.A.

(*First received* 15 *May* 1987 *and in final form* 15 *October* 1987)

Abstract—Evidence is presented that interior surfaces of a state-of-the-art emissions test chamber can act as a transient sink for organic emissions. The major contribution of this paper is to present a class of mechanistic, mathematical models which accounts for this phenomenon as well as the effect of increasing chamber concentration on the emission rate of the source. A key point is that the effect of the chamber sink can be adjusted out simply by first fitting the appropriate model, then setting to zero the rate constant which governs sink adsorption–absorption. As a consequence of this mathematical development, a source emission rate as a function of time and a steady-state emission rate factor are given precise definitions. Applications involve modeling 1,4-dichlorobenzene emission from moth crystal cake, and mixed emissions from latex caulk. In the first case, at a low air exchange rate and low humidity, the repressive effect of increasing vapor pressure tends to overshadow the sink effect. Increased humidity tends to offset the increase in emission rate which otherwise would occur with increased air exchange. Temperature is the principal determinant of the steady-state emission rate. For the latex caulk, the effect of a sink is to retard the apparent emission rate but lengthen the period of emissions.

Key word index: Chamber testing, sink effect, latex caulk, moth crystal, organic emissions, mathematical models, emission rate function, emission rate factor.

1. INTRODUCTION

The purpose of this paper is to present a variety of extensions to a class of mechanistic, time-dependent models proposed by Dunn (1987) which mathematically decouple the true emission characteristics of an organic source from "coloration" imposed by an emissions test chamber. Based on empirical evidence of a longer than expected residue of emissions, Dunn's model incorporated a term for an adsorptive wall effect whose release rate was assumed to be equal to that of the original source. The value of this approach is that it allowed not only generation of a curve representing actual concentration in the chamber over time, but produced an additional curve, obtained by setting the adsorptive rate constant to zero, which represented the theoretical concentration in the chamber had there been no wall effect.

In keeping with the distinction proposed by Dunn, the models treated here are thought to apply to thin film sources, as distinguished from deep sources whose emission rates are diffusion limited. First, in line with the terminology established by Renes *et al.* (1985), we have generalized the specific concept of a wall effect to the general notion of a sink effect, whether it be actual wall or conduit adsorption, absorption by a gasket seal, or even accumulation in an unventilated portion of the chamber. In a more sophisticated experiment involving binary composite materials, one element might serve as a sink for emissions from the other, e.g. a linoleum layer when testing emissions from its adhesive. Our assumption differs slightly from that of Renes *et al.* in that our sink has the capability of releasing adsorbed material; whereas, from the form of the model shown, their sink is irreversible. Second, by including an additional rate constant, we have relaxed the assumption that the release rate from the sink is equal to that from the original source. It is very likely that a different mechanism would be involved. Third, we have introduced yet another rate constant to reflect the potential effect of chamber concentration on the emission rate of the source. Fourth, we have distinguished between thin film models which represent concentration for a decreasing source (e.g. a swatch of floor wax or carpet glue on an inert carrier) and constant source models (e.g. as might be obtained by use of permeation tubes or, in our case, a cake of moth crystal).

Since the adsorptive properties of typical indoor surfaces now have been documented by Renes *et al.* (1985) for NO_2 and SO_2 and by Seifert and Schmahl (1987) for selected organics, the approach which we

NTIS is authorized to reproduce and sell this report. Permission for further reproduction must be obtained from the copyright owner.

visualize is to start with an appropriate mathematical model, replace whatever sink effects characterize the test chamber with those sink effects which characterize a living–working environment, and then use the model to predict the actual exposure level. Results are given of a reanalysis, based on these new models, of the latex caulk data previously reported by Dunn (1987). Also treated in some detail are the moth crystal emissions data which are discussed by Nelms *et al.* (1987). All emissions data were obtained in the 166 ℓ, stainless-steel test chamber described by Sanchez *et al.* (1987). Its interior had been electropolished after assembly; all conduits were either Teflon or Pyrex glass.

2. GENERAL FORM OF THIN FILM MODELS

As visualized here, a test chamber operating system consists of four (mathematical) compartments; namely, the source, the well-mixed contents of the chamber, an exit, and a sink. Rate constants describe the flow among these compartments, as illustrated by the following scheme:

$$\begin{array}{ccccc} & & \text{Sink } (w) & & \\ & & k_3 \uparrow\downarrow k_4 & & \\ \text{Source } (A) & \underset{k_2}{\overset{k_1}{\rightleftharpoons}} & \text{Chamber } (x-y-w) & \xrightarrow{k_2} & \text{Exit } (y), \end{array}$$

where

A is initial mass to be emitted by the source, $x = x(t)$ is mass emitted to the chamber by time t, $y = y(t)$ is mass exiting from the chamber by time t, $w = w(t)$ is mass in the sink at time t.

It follows that the concentration in the chamber at time t is given by $C(t) = (x - y - w)/V$, where V is the chamber volume, and $I(t_1, t_2) = y(t_2) - y(t_1)$ is the mass leaving the chamber in the time interval (t_1, t_2). Clearly, $y(t) = I(0, t)$, assuming $y(0) = 0$. We postulate that, in a well-mixed chamber, the system is described adequately by the following set of ordinary differential equations:

$$\frac{dx}{dt} = k_1 g(x, t) - k_2(x - y - w), \tag{1}$$

$$\frac{dy}{dt} = k_2(x - y - w), \tag{2}$$

$$\frac{dw}{dt} = k_3(x - y - w) - k_4 w. \tag{3}$$

Physically, the right-hand side of Equation (1) defines the emission rate (ER) of the source at any time t. It states that the rate of introduction of material into the chamber is proportional to some function, $g(x, t)$, of time and the amount already emitted, while being inhibited by increasing mass, or equivalently, concentration in the vapor phase of the chamber. A precise definition of the emission rate factor can then be given, namely

$$\text{Emission rate factor (ERF)} = \lim_{t \to \infty} \frac{dx}{dt}, \tag{4}$$

representing the steady-state rate of mass introduction from the source into the chamber atmosphere. Equation (2) states that the emission rate from the chamber is proportional to the mass in the chamber, or equivalently the chamber concentration since the chamber volume is constant. Equation (3) states that the rate at which material moves to the sink is proportional to the mass (or concentration) in the chamber, while the rate of removal from the sink is proportional to the amount already in the sink. Both rate constants, k_1 and k_2, are required to describe the source. The rate of movement to the sink is described by the rate constant k_3, and the rate of release from the sink is described by k_4. Presumably, values of k_3 and k_4 which characterize the test chamber differ drastically from those which would be associated with an actual living–working environment. Assuming a constant air flow rate, F, through the chamber, then $k_2 = F/V$, the number of air changes per unit time. We assume that F is specified by the experimenter so that k_2 is a known rate constant.

The next section describes physical models which are obtained as solutions of the above set of equations. Solutions with $k_3 \neq 0$ and $k_4 \neq 0$ are referred to as full models. Solutions with $k_3 \neq 0$ but $k_4 = 0$ are sink models, since the rate of emission from the source is not then affected by increasing chamber concentration. Conversely, solutions with $k_3 = 0$ and $k_4 \neq 0$ are called vapor pressure (VP) models, and represent the absence of a sink. However, VP models play a dual role, as noted by Dunn (1987), in the sense that they are indistinguishable from sink models in which $k_3 = k_4$ and $k_4 = k_1$; i.e. where the rate constant for removal from the sink is identical to that for the original source. If both $k_3 = 0$ and $k_4 = 0$, then the result is called simply a dilution model.

3. PHYSICAL MODELS FOR EMISSIONS

3.1. *Constant source models*

Suppose we have a source which acts as if it were a constant emitter, at least for a finite period of time. A permeation tube exhibits this behavior; a source such as moth crystal cake whose emission rate is limited by its surface area also behaves this way to a good approximation. Thus $A = \infty$ effectively, and, if we suppose that the potential for emissions is constant during this period, then $g(x, t) = 1$ in Equation (1). Table 1 shows the four different solutions of Equations (1)–(3) under these assumptions, given that the chamber concentration is negligible at time zero. Clearly, these are related. The full model reduces smoothly to either the sink model as $k_4 \to 0$ or the VP model as $k_3 \to 0$. If both $k_3 = 0$ and $k_4 = 0$, then all models reduce to the simple dilution model.

The limiting forms of these models as $t \to \infty$ are given in Table 2. Note the intuitive result that the limiting steady-state chamber concentration for the

Table 1. Constant source models, showing the chamber concentration, $C(t)$, mass in the sink, $w(t)$, and mass $I(t_1, t_2)$ emitted from the chamber from time t_1 to time t_2. $L(k_3) = 0$ if $k_3 = 0$; otherwise $L(k_3) = 1$

Full model ($k_3 \neq 0$, $k_5 \neq 0$).

$$C(t) = k_1 k_2 [(k_4 - r_2)^2 (1 - e^{-r_2 t})/s_2 + L(k_3)(k_4 - r_3)^2 (1 - e^{-r_3 t})/s_3]/V, \quad (5)$$

$$w(t) = k_1 k_2 k_3 [(k_4 - r_2)(1 - e^{-r_2 t})/s_2 + (k_4 - r_3)(1 - e^{-r_3 t})/s_3], \quad (6)$$

$$I(t_1, t_2) = k_1 k_2 (t_2 - t_1)/s_1 + k_1 k_2 (k_4 - r_2)[(k_5 - r_2)(k_3 + k_4 - r_2) - k_3 k_5](e^{-r_2 t_1} - e^{-r_2 t_2})/(r_2 s_2) + L(k_3) k_1 k_2 (k_4 - r_3)[(k_5 - r_3)(k_3 + k_4 - r_3) - k_3 k_5](e^{-r_3 t_1} - e^{-r_3 t_2})/(r_3 s_3), \quad (7)$$

$$r_2, r_3 = \{k_2 + k_3 + k_4 + k_5 \pm [(k_2 + k_3 + k_4 + k_5)^2 - 4k_4(k_2 + k_5)]^{1/2}\}/2,$$

$$s_1 = k_2 + k_5,$$

$$s_i = k_2 k_5 (k_4 - r_i)^2 + k_2 k_3 r_i^2 + [(k_5 - r_i)(k_3 + k_4 - r_i) - k_3 k_5)]^2, \text{ for } i = 2, 3.$$

Sink model ($k_3 \neq 0$, $k_5 = 0$).

$$C(t) = k_1 [(r_1 - k_4)(1 - e^{-r_1 t})/r_1 - (r_2 - k_4)(1 - e^{-r_2 t})/r_2]/[(r_1 - r_2)V], \quad (8)$$

$$w(t) = k_1 k_3 [(1 - e^{-r_2 t})/r_2 - (1 - e^{-r_1 t})/r_1]/(r_1 - r_2), \quad (9)$$

$$I(t_1, t_2) = k_1 \{(r_1 - k_3 - k_4)[r_1(t_2 - t_1) + e^{-r_1 t_2} - e^{-r_1 t_1}]/r_1 - (r_2 - k_3 - k_4)[r_2(t_2 - t_1) + e^{-r_2 t_2} - e^{-r_2 t_1}]/r_2\}/(r_1 - r_2), \quad (10)$$

$$r_1, r_2 = \{k_2 + k_3 + k_4 \pm [(k_2 + k_3 + k_4)^2 - 4k_2 k_4]^{1/2}\}/2.$$

VP model ($k_3 = 0$, $k_5 \neq 0$).

$$C(t) = k_1 [1 - e^{-(k_2 + k_5)t}]/[(k_2 + k_5)V], \quad (11)$$

$$I(t_1, t_2) = k_1 k_2 (t_2 - t_1)/(k_2 + k_5) - k_1 k_2 [e^{-(k_2 + k_5)t_1} - e^{-(k_2 + k_5)t_2}]/(k_2 + k_5)^2. \quad (12)$$

Dilution model ($k_3 = 0$, $k_5 = 0$).

$$C(t) = k_1 (1 - e^{-k_2 t})/(k_2 V) \quad (13)$$

$$I(t_1, t_2) = k_1 [k_2 (t_2 - t_1) + e^{-k_2 t_2} - e^{-k_2 t_1}]/k_2. \quad (14)$$

Table 2. Steady-state chamber concentration and mass in the sink, corresponding to the constant source models listed in Table 1

	Concentration, $C(\infty)$	Sink, $w(\infty)$
Full model*	$k_1 k_2 [(k_4 - r_2)^2/s_2 + (k_4 - r_3)^2/s_3]/V$	$k_1 k_2 k_3 [(k_4 - r_2)/s_2 + (k_4 - r_3)/s_3]$
Sink model	$k_1/(k_2 V)$, independent of k_3 and k_4	$k_1 k_3/(k_2 k_4)$
VP model	$k_1/[(k_2 + k_5)V]$	0
Dilution model	$k_1/(k_2 V)$	0

*r_2, r_3, s_2, and s_3 are as defined in Table 1.

sink model is identical to that of the dilution model; i.e. independent of the magnitude of any sink effect.

Theoretical forms of emission rate factors, as defined by Equation (4), are given in Table 3. Again, there is nothing to distinguish between the sink and dilution models. Note that the ERF for the VP model will always be less than that for the sink model to the extent that $k_5 > 0$.

The application of these principles is the central theme of this paper. Figure 1 illustrates the forms taken by equations in Table 1. Using 24.08 g of moth crystal cake as the source, 1,4-dichlorobenzene concentrations were measured in the test chamber, maintained at 35.6°C (SD = 0.10), 50.3% r.h. (SD = 9.4), and $k_2 = 0.25$ air changes h^{-1} (ACH), and the results are plotted as +s. A least squares fit of the sink model, using SAS procedure NLIN (1985), resulted in estimates $k_1 = 259$ mg h^{-1} (SE = 8.32), $k_3 = 0.128$ h^{-1} (SE = 0.0196), and $k_4 = 0.0802$ h^{-1} (SE = 0.0105). The solid line in Fig. 1 is a plot of the fitted model, and is our best estimate of the actual, dynamic concentration in the chamber. The dashed line (– –), obtained by setting $k_3 = 0$, represents our best assessment of the concentration which would have resulted had there been no sink effect. The full model gave an equally good fit (cf. Table 5, test 10.1), but appeared to be overparameterized by the presence of k_5.

As a general principle: The proper way to remove a sink effect mathematically is to fit either the sink model or the full model, depending on whether or not there is

Table 3. Theoretical emission rate factors for constant source models

Full model*	$ERF = k_1 \{1 - k_2 k_5 [(k_4 - r_2)^2/s_2 + (k_4 - r_3)^2/s_3]\}$
Sink and dilution models	$ERF = k_1$
VP model	$ERF = k_1 k_2/(k_2 + k_5)$

*r_2, r_3, s_2, and s_3 are as defined in Table 1.

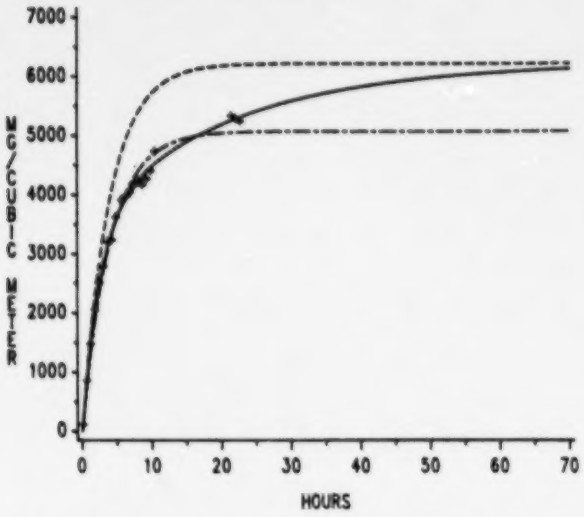

Fig. 1. 1,4-Dichlorobenzene emission from moth crystal at 36°C, 50% r.h. and 0.25 ACH. Sink ——, sink ($k_3 = 0$) – – –, dilution — – —.

statistical evidence that $k_3 = 0$ (e.g. by examination of its standard error or confidence interval), then setting $k_3 = 0$ in the resulting fitted model.

Note that the dashed line in Fig. 1 is not the same as that which would have resulted had the dilution model been fitted directly. In fact, the least squares fit of the dilution model and that of the VP model were the same, $k_1 = 211$ mg h^{-1} (SE = 8.26) and $k_3 = 0$ being estimated for the latter. The result is plotted in Fig. 1 as the dot–dash (–··–) line. It does not appear to fit as well as the sink model, particularly the last three data points. Using formulae from Table 2, estimated steady-state concentrations are 6230 mg m^{-3} for the sink model and 5080 mg m^{-3} for the VP-dilution model. If the sink model is correct, then an unwary experimenter who felt that the last three data points represented steady state would underestimate that value by about 15%.

From Table 3, the emission rate factors are equal to the respective k_1 estimates. These are also the emission rates, dx/dt, since k_3 is assumed to be zero in the sink model and was estimated to be zero in the VP model.

3.2. *Decreasing source models*

Suppose that $A < \infty$, and that $g(x, t) = (A - x)$ in Equation (1). Physically, this is an assumption that the source emission rate is proportional to the amount remaining to be emitted, while being inhibited in proportion to the chamber concentration. With Equations (2) and (3) remaining unchanged, the four possible models, obtained as solutions of Equations (1)–(3) and corresponding to those in Table 1, are listed in Table 4. Again, we have assumed that the chamber concentration is negligible at time zero.

For all models listed in Table 4, both $C(t)$ and $w(t)$ decay to zero at $t \to \infty$. Also, since $x = y = A$ in the limit, the emission rate factors are zero for all models. The implications of these properties will be discussed in the next section in connection with examples of the analysis of mixed emissions from latex caulk.

4. EVIDENCE FOR A CHAMBER SINK EFFECT

4.1. 1,4-*Dichlorobenzene emission from moth crystal cake*

Experimental conditions for 13 emissions tests of moth crystal cakes (Nelms *et al.*, 1987) are given in Table 5 in the order actually used in the laboratory. The chamber was cleaned between each test as described by Sanchez *et al.* (1987), followed by a background check. The sample size, N, refers to the number of separate determinations of chamber concentration made during each test. The four constant source models were fitted to each data set using SAS (1985) procedure NLIN, and the residual sums of squares (SSE) are listed in Table 5 as a basis for choosing the most appropriate model. $C(t)$ forms were fitted since the data were obtained as virtually instantaneous measurements of chamber concentration.

In most cases, the least squares fit of the full model converged to a solution in which either $k_3 = 0$ or $k_3 = 0$ (or both). This is indicated in the column "Full". Where all parameter estimates were positive for the full model, the residual SSE is listed explicitly. Even then, except for test 10.1, huge standard errors associated with the estimates suggested that the full model was overparameterized. Only for test 10.1 was SSE smaller than that listed for either the sink or the VP model, and then only minimally. In this case, k_3 was significantly greater than zero, but not k_3, so that the sink model seemed preferred. There appear to have been major

Table 4. Decreasing source models, showing the chamber concentration, $C(t)$, mass in the sink, $w(t)$, and mass $I(t_1, t_2)$ emitted from the chamber from time t_1 to time t_2

Full model ($k_3 \neq 0$, $k_5 \neq 0$).

$$C(t) = A \sum_{i=1}^{3} s_i r_i (k_1 - r_i) e^{-r_i t}/(DV), \tag{15}$$

$$w(t) = A \sum_{i=1}^{3} s_i [r_i^2 - (k_1 + k_2 + k_3) r_i + k_1 k_2] e^{-r_i t}/D, \tag{16}$$

$$I(t_1, t_2) = k_2 A \sum_{i=1}^{3} s_i (r_i - k_1)(e^{-r_i t_2} - e^{-r_i t_1})/D, \tag{17}$$

$$D = k_1 k_2 k_3 \{r_1 (r_2^2 - r_3^2) + r_2 (r_3^2 - r_1^2) + r_3 (r_1^2 - r_2^2)\},$$
$$s_1 = (r_3 - r_2)\{r_2 r_3 (k_2 + k_3) - k_1 k_2 (r_2 + r_3 - k_1)\},$$
$$s_2 = (r_1 - r_3)\{r_1 r_3 (k_2 + k_3) - k_1 k_3 (r_1 + r_3 - k_1)\},$$
$$s_3 = (r_2 - r_1)\{r_1 r_2 (k_2 + k_3) - k_1 k_3 (r_1 + r_2 - k_1)\},$$

and r_1, r_2, and r_3 are roots of

$$r^3 - (k_1 + k_2 + k_3 + k_4 + k_5) r^2 + [k_2 (k_1 + k_4) + k_1 (k_3 + k_4) + k_4 k_5] r - k_1 k_2 k_4 = 0.$$

Sink model ($k_3 \neq 0$, $k_5 = 0$).

$$C(t) = k_1 A \{(k_4 - k_1) e^{-k_1 t}/[(r_1 - k_1)(r_2 - k_1)] - (k_2 + k_3 - r_2) e^{-r_2 t}/[(r_1 - r_2)(r_1 - k_1)] + (k_2 + k_3 - r_1) e^{-r_1 t}/[(r_1 - r_2)(r_2 - k_1)]\}/V, \tag{18}$$

$$w(t) = A(k_2 - r_1)(k_2 + k_3 - r_2)\{r_1 (1 - e^{-k_1 t}) - k_1 (1 - e^{-r_1 t})\}/[r_1 (r_2 - r_1)(r_1 - k_1)] - A(k_2 - r_2)(k_2 + k_3 - r_1)\{r_2 (1 - e^{-k_1 t}) - k_1 (1 - e^{-r_2 t})\}/[r_2 (r_2 - r_1)(r_2 - k_1)], \tag{19}$$

$$I(t_1, t_2) = A k_2 (k_4 - k_1)(e^{-k_1 t_1} - e^{-k_1 t_2})/[(r_1 - k_1)(r_2 - k_1)] - A k_1 k_2 (k_2 + k_3 - r_2)(e^{-r_2 t_1} - e^{-r_2 t_2})/[r_1 (r_1 - r_2)(r_1 - k_1)] + A k_1 k_2 (k_2 + k_3 - r_1)(e^{-r_1 t_1} - e^{-r_1 t_2})/[r_2 (r_1 - r_2)(r_2 - k_1)], \tag{20}$$

$$r_2, r_3 = \{k_2 + k_3 + k_4 \pm [(k_2 + k_3 + k_4)^2 - 4 k_2 k_4]^{1/2}\}/2.$$

VP model ($k_3 = 0$, $k_5 \neq 0$).

$$C(t) = k_1 A (e^{-r_2 t} - e^{-r_1 t})/[(r_1 - r_2) V], \tag{21}$$

$$I(t_1, t_2) = A[r_1 (e^{-r_2 t_1} - e^{-r_2 t_2}) - r_2 (e^{-r_1 t_1} - e^{-r_1 t_2})]/(r_1 - r_2), \tag{22}$$

$$r_1, r_2 = \{k_1 + k_2 + k_5 \pm [(k_1 + k_2 + k_5)^2 - 4 k_1 k_2]^{1/2}\}/2.$$

Dilution model ($k_3 = 0$, $k_5 = 0$).

$$C(t) = k_1 A (e^{-k_2 t} - e^{-k_1 t})/[(k_1 - k_2) V], \tag{23}$$

$$I(t_1, t_2) = A[k_1 (e^{-k_2 t_1} - e^{-k_2 t_2}) - k_2 (e^{-k_1 t_1} - e^{-k_1 t_2})]/(k_1 - k_2). \tag{24}$$

Table 5. Lack-of-fit (SSE) comparisons of all constant source models applied to 1,4-dichlorobenzene emissions from moth crystal cake

Test	Temp. (°C)	r.h. (%)	ACH (= k_2)	N	Full (SSE)	Sink (SSE)	VP (SSE)	Dilution (SSE)
3	23.4	15.2	0.98	13	2410	2410(11)*	(= Dilution)	24015
4	23.2	14.9	0.50	14	16304	16304(12)*	(= Dilution)	89780
7	23.3	19.3	0.29	22	(= VP)	(= Dilution)	37144(20)*	50573
5.1	23.3	17.5	0.50	17	(= VP)	(= Dilution)	14282(15)*	17557
6.1	22.8	51.7	0.26	18	(= Dilution)	62938(15)*	(= Dilution)	68051
8.1	22.6	53.1	0.99	16	(= Dilution)	2583(13)*	(= Dilution)	6339
9	35.5	14.8	0.27	16	1462778	2384895	1462777(14)*	2385391
10	35.6	34.0	0.25	16	(= VP)	(= Dilution)	1639028(14)*	2200353
10.1	35.6	50.3	0.25	21	147658	147762(18)*	(= Dilution)	676431
11	35.4	18.1	0.99	18	96923	96923(16)*	(= Dilution)	108483
12	36.3	49.7	1.92	10	(= Sink)	17642(7)*	(= Dilution)	65913
13	35.4	54.8	0.49	13	(= VP)	549251	415228(11)*	577399
14	24.8	42.5	1.92	10	669	1738	669(8)*	1821

* Preferred model.

sink effects for tests 3, 4, 10.1, and 12, and, to a lesser extent, for tests 6.1, 8.1, and 11, though k_3 was not significantly different from zero in the sink model for the latter cases. This is substantiated by the fact that Nelms *et al.* (1987) recovered 160 and 23 mg of 1,4-dichlorobenzene from the chamber walls at the end of tests 10.1 and 11, respectively. The vapor pressure term, k_5, was significantly greater than zero for tests 7, 9, and 14, but not for tests 5.1, 10, and 13. The simple dilution model did not seem to be adequate in any case.

A general pattern is difficult to discern. These tests were dominated by either a sink effect or a vapor pressure effect, but not by both simultaneously. Two physical explanations are suggested. Table 6 shows estimates of steady-state chamber concentrations and emission rate factors for the 13 tests, based on

Table 6. Steady-state concentrations and emission rate factors for 1,4-dichlorobenzene from moth crystal cake (SE = standard error)

Test	Sample wt (g)	Model	Steady state Est. ($mg\ m^{-3}$)	Steady state SE ($mg\ m^{-3}$)	ERF sample^{-1} Est. ($mg\ h^{-1}$)	ERF sample^{-1} SE ($mg\ h^{-1}$)	ERF g^{-1} Est. ($mg\ h^{-1}\ g^{-1}$)	ERF g^{-1} SE ($mg\ h^{-1}\ g^{-1}$)	ERF cm^{-2} Est. ($mg\ h^{-1}\ cm^{-2}$)	ERF cm^{-2} SE ($mg\ h^{-1}\ cm^{-2}$)
3	24.1	Sink	552	6.95	89.8	1.13	3.72	0.047	1.63	0.021
4	24.6	Sink	986	24.0	81.9	1.99	3.33	0.081	1.49	0.036
7	29.0	VP	1230	14.5	59.2	0.70	2.04	0.024	1.08	0.013
		($k_s = 0$)	(1390	56.5)	(66.8	2.72)	(2.03	0.094)	(1.21	0.049)
5.1	29.3	VP	1060	11.4	88.2	0.94	3.01	0.025	1.60	0.017
		($k_s = 0$)	(1160	49.4)	(96.4	4.10)	(3.29	0.140)	(1.75	0.075)
6.1	29.1	Sink	1610	82.9	69.5	3.58	2.39	0.123	1.26	0.065
8.1	26.8	Sink	543	5.23	89.2	0.86	3.34	0.032	1.62	0.016
9	21.7	VP	5220	135	234	6.06	10.8	0.279	4.25	0.110
		($k_s = 0$)	(6870	600)	(308	26.9)	(14.2	1.24)	(5.60	0.489)
10	25.3	VP	5440	158	226	6.54	8.91	0.258	4.11	0.119
		($k_s = 0$)	(6720	581)	(279	24.1)	(11.0	0.951)	(5.07	0.438)
10.1	24.1	Sink	6230	200	259	8.32	10.7	0.346	4.70	0.151
11	23.9	Sink	1740	23.8	286	3.91	12.0	0.164	5.20	0.071
12	28.2	Sink	1050	40.5	334	12.9	11.9	0.458	6.08	0.235
13	29.7	VP	2970	79.2	242	6.44	8.12	0.217	4.39	0.117
		($k_s = 0$)	(3720	386)	(302	31.4)	(10.2	1.06)	(5.50	0.571)
14	28.4	VP	308	3.36	98.1	1.07	3.46	0.038	1.78	0.019
		($k_s = 0$)	(399	26.5)	(127	8.44)	(4.48	0.297)	(2.31	0.153)

matching the preferred models indicated in Table 5 with their corresponding computational formulae in Tables 2 and 3. Within each temperature octave, choice of the VP model over the sink model generally corresponded to those tests with high chamber concentrations, i.e. tests 7, 5.1, 9, 10, and 13. This is consistent with a vapor pressure gradient theory proposed by Nelms *et al.* (1987). The sink model was preferred if either the concentration was relatively low (tests 3, 4, 8.1, 11, and 12), or the r.h. was high (tests 6.1 and 10.1). A finite adsorption capacity by the walls could have accounted for a greater fraction of the emissions in the first case; additional humidity might have conditioned the adsorptive sites by some mechanism in the second case. Test 14 was the exception to both rules, the VP model being preferred even though the concentration was low and the humidity high.

Alternatively, based on the dual role of the VP model, it may be that the apparent vapor pressure effect represents only a gradation of the sink effect which was dominant in other tests. With this possibility in mind, Table 6 shows (in parentheses) recalculated estimates obtained by setting $k_s = 0$ in the VP estimation formulae of Tables 2 and 3. In effect, we have treated the VP model as a special form of sink model, then removed the sink effect mathematically. For comparable tests 4 and 5.1, the net effect was to move estimates of the ERF on a g^{-1} basis into closer alignment while the similarity between steady-state estimates decreased. Both estimates for test 10 moved closer to those for test 10.1. Revised estimates for test 13 also seem more in line with those for test 10.1.

In spite of the modest improvements noted above, we believe that both a wall effect and a vapor pressure effect always were present in the chamber. Analyzing the leachate from the chamber walls after every test might have provided a definitive answer, but this was not done. We suggest that the preferred models indicated in Table 5 represent the dominant effects, depending on the test conditions, and that the data were insufficient to support estimation of the lesser effect in all cases except test 10.1. This test was the basis of Fig. 1.

In order to summarize the results of Table 6 based on this conclusion, we used Stepwise Regression (1985) to construct empirical models relating steady-state chamber concentration and ERF on a g^{-1} basis to selected functions of temperature (T), r.h., and air exchange rate (ACH). The list of functions made available included all products, all reciprocals, all logarithms, and ratios of all pairs of T, r.h., and ACH. The models selected are:

$$\text{Steady state } (mg\ m^{-3}) = 225.1 - 1585/\text{ACH} + 83.56\,T/\text{ACH}, (R^2 = 0.990) \quad (25)$$

$$\text{ERF } (mg\ h^{-1}\ g^{-1}) = -12.28 + 0.6155\,T + 32.38\,\text{ACH/r.h.}, (R^2 = 0.954). \quad (26)$$

All coefficients were significant at the 0.05 level (or less) to be included. These functions are plotted as response surfaces in Figs 2–4, respectively.

Each contour in Fig. 2 indicates how ACH must be adjusted to compensate for increasing temperature in order to maintain a constant chamber concentration. Clearly, the chamber concentration of dichlorobenzene builds up more rapidly at high temperatures with decreasing ACH than at low temperatures. These features seem to hold regardless of the humidity level,

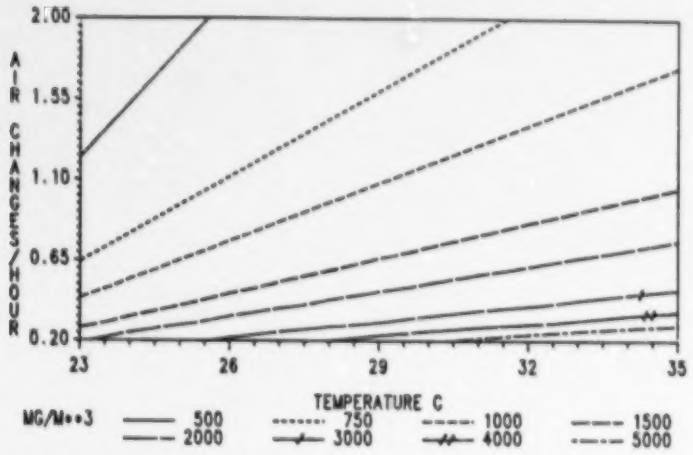

Fig. 2. Steady-state concentration of 1,4-dichlorobenzene from moth crystal cake.

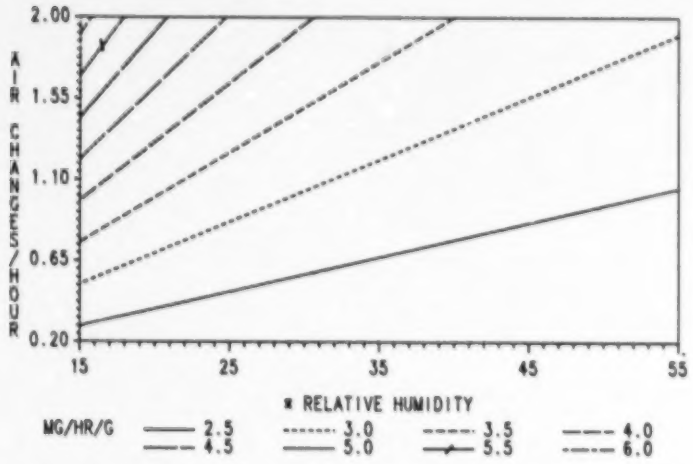

Fig. 3. Emission rate factor for 1,4-dichlorobenzene from moth crystal cake at 23°C.

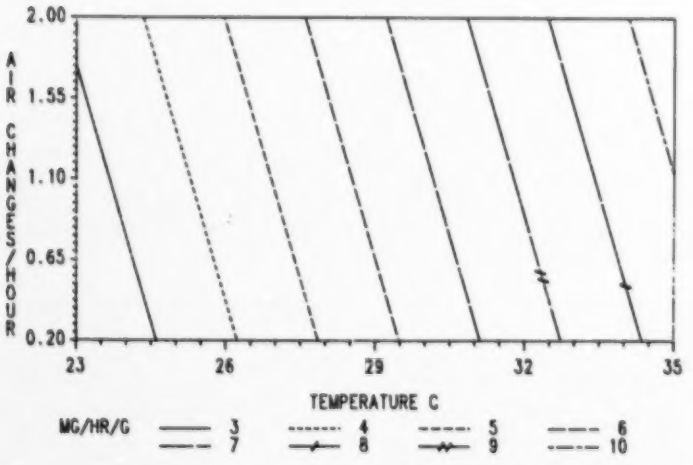

Fig. 4. Emission rate factor for 1,4-dichlorobenzene from moth crystal cake at 50% r.h.

since no function of r.h. was selected for inclusion in Equation (25) by the stepwise procedure.

The dependence of ERF on the reciprocal of RH resembles that of the Berge equation (Godish and Rouch, 1985). The effect of r.h. at $T = 23°C$ is shown in Fig. 3. Each contour reflects how the ACH must be adjusted to compensate for increasing r.h. in order to maintain a constant ERF on a g^{-1} basis. Increasing ACH will increase the ERF more rapidly at low r.h. than at high RH. Increasing r.h. will offset the effect of increasing ACH, particularly at high ACH values. These relationships appear to hold over the temperature range used here, since T occurs only linearly in Equation (26). Based on the same equation, Fig. 4 shows the effect of temperature variation at 50% r.h. Clearly, temperature was the major determinant of ERF over the range of experimental conditions used in these tests. The near-vertical appearance of the contours suggests that ACH has only a limited effect on ERF at any temperature setting.

Based on our repeated observation of the tendency of 1,4-dichlorobenzene concentrations to rise smoothly to a steady-state level, we strongly maintain that moth crystal cake emission is a surface phenomenon. Hence, we would have preferred to express ERF on a cm^{-2} surface area basis rather than a g^{-1} basis. However, we could not do this because individual surface areas were not measured; only an average value of $55\ cm^2$ was calculated from the geometry of the moth crystal cakes. Since the weight values shown in Table 6 reflect considerable variation in the actual sample sizes, Figs 3 and 4 most accurately represent ERF relationships, considering this limitation of the data set.

4.2. *Mixed emissions from latex caulk*

In previous work, Dunn (1987) reported fits of the VP model to emissions from a commercial latex caulk. However, the VP model was treated there as a model for "wall effects", whose influence could be removed mathematically as we have done here. Since then, we have derived the more general form of sink model shown in Table 4, as well as its full model counterpart. Table 7 compares the residual sums of squares obtained from a least squares fit of each of the four decreasing source models using SAS (1985) procedure NLIN. $I(t_1, t_2)$ forms were fitted since the data were obtained by accumulations over time intervals in Tenax samplers.

There is statistically significant evidence that both a sink effect and a vapor pressure effect were active for emission of butyl propionate at both ACH levels, and for methyl ethyl ketone emission at high ACH. For methyl ethyl ketone at low ACH, k_3 in the VP model was significantly greater than zero while k_3 in the sink model was not significant, even though both models fitted equally well. Therefore, we conclude that methyl ethyl ketone emission was limited by the chamber concentration at both air exchange rates, but the wall effect only became apparent at the high ACH. An explanation is suggested in Table 8, which lists least squares estimates of the rate constants for the full model. The rate constant k_4 exceeds k_3 by two orders of magnitude at low ACH, but only by a factor of four at high ACH. At low ACH, the walls were able to maintain equilibrium with a slowly decreasing chamber concentration, but at high ACH removal from the walls lagged behind. We believe that the same argument accounts for the appearance of a wall effect for

Table 7. Lack-of-fit (SSE) comparisons of all decreasing source models fitted to emissions from latex caulk at 23°C and 50% r.h.

	ACH = 0.361, $N = 12$				ACH = 1.85, $N = 9$			
	Full	Sink	VP	Dilution	Full	Sink	VP	Dilution
Total organics	18.2	20.9	37.1	72.1	282	282	412	479
Methyl ethyl ketone	0.430	0.583	0.582	0.603	0.583*	4.04	4.08	4.66
C_8 alcohol	9.78	12.0	12.0	15.1	28.6	33.8	68.1	77.5
Butyl propionate	0.912*	2.66	2.66	2.92	4.63*	14.9	15.2	17.5

* Significantly better fit than all other models ($\alpha = 0.05$).

Table 8. Rate constant estimates for the decreasing source, full model fitted to latex caulk emissions at 23°C and 50% r.h.

	ACH ($= k_2$)	A ($\mu g\ g^{-1}$)	k_1 (h^{-1})	k_3 (h^{-1})	k_4 (h^{-1})	k_5 (h^{-1})
Total organics	0.361	604	0.746	0.440	0.167	5.55×10^{-5}
	1.85	856	0.891	1.79	0.0457	1.93×10^{-3}
Methyl ethyl ketone	0.361	84.8	2.62	49.1	4238	0.268
	1.85	105	5.44	9.30	40.9	0.389
C_8 alcohol	0.361	199	1.00	168	221	0.322
	1.85	283	0.734	2.10	0.0881	2.66×10^{-3}
Butyl propionate	0.361	82.2	1.07	794	1896	0.238
	1.85	97.0	3.00	14.0	6.72	0.0145

C_8 alcohol at high ACH, when none is apparent at low ACH. Again, a comparison of the k_3 and k_4 estimates is informative.

Even though the sink model fitted the total organics data almost as well as the full model, the fact that individual compounds exhibited both sink and vapor pressure effects suggests that the latter should be used. Both k_3 in the sink model and k_3 in the VP model were significantly greater than zero at both ACH levels when these models were fitted separately to the data. Unfortunately, estimating five parameters in the full model based on a limited number of data points often led to highly correlated estimates; so much so, in fact, that the information matrix was nearly singular, and unreasonably large standard errors were produced. This is why standard errors are not listed in Table 8. Hence, in future work with these models, we suggest fitting the simpler models first, then making comparisons to the fit of the full model using the SSE criterion as we have done.

Estimates of A in Table 8 are expressed as μg of emittable material g^{-1} of source. We use this fact to illustrate the application of these models in adjusting out any generic sink effect. Suppose that 5 g of latex caulk were introduced into the chamber, maintained at 23°C and 50% r.h., with 1.85 ACH. The appropriate full model for the chamber concentration of butyl propionate is Equation (15), with $A = 5 \times 97.0 = 485$ μg sample^{-1}, and rate constants taken directly from Table 8. Mass $[= C(t) \times 0.166]$ in the vapor phase of the chamber rather than concentration has been plotted as a solid line in Fig. 5. The theoretical mass, had there been no sink effect, is plotted as the dot–dash line (– · –), and was obtained by setting $k_3 = 0$ in Equation (15). Thus, the transient sink effect of the walls would be to reduce peak concentration by about 50%. The mass on the walls, obtained from Equation (16), is plotted as the dashed line (– –). Note that its response in the chamber is somewhat delayed compared with that of the vapor phase curves. Note also that at its peak, the wall effect accounted for nearly twice the mass of that in the vapor phase. This is the most extreme case of those listed in Table 8, but clearly it contradicts the notion that a state-of-the-art emissions test system automatically will be non-adsorptive. In order to complete a description of the butyl propionate emissions, its chamber-based emission rate function, $dx/dt = k_1[A - VC(t) - I(0, t) - w] - k_3 VC(t)$, as defined by Equation (1), is plotted as the solid line in Fig. 6. The theoretical rate function, had there been no wall effect and obtained by setting $k_3 = 0$ in dx/dt, is plotted as the dashed (– –) line. Again the difference is striking. The material coming off the walls was able to contribute to the vapor pressure effect, thereby suppressing source emissions and leading to a relatively sustained emission rate. This effect only emerged after the initial "explosion" of butyl propionate essentially had been removed from the chamber, i.e. after about $3\frac{1}{2}$ h. Both emission rate functions are tending toward zero, as predicted by theory.

5. SUMMARY AND CONCLUSIONS

In spite of meticulous care in chamber design, construction, and operation, we have presented evidence that a state-of-the-art emissions test chamber can act as a transient sink. At a low air exchange rate, particularly at low humidity, the expression of this effect may be obscured by the other main effect in the chamber; namely, that of increased concentration as it affects the emission rate of the source. We have termed this the vapor pressure (VP) effect. We feel that a major contribution of this paper has been to present a class of mathematical models which accounts for both phenomena. The source emission rate (ER) as a function of time and the steady state, emission rate

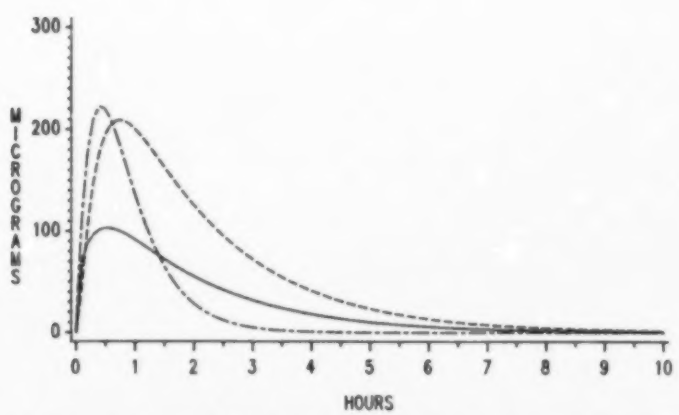

Fig. 5. Butyl propionate emission from latex caulk at 23°C, 50% r.h., and 1.85 ACH. Chamber ——, chamber ($k_3 = 0$) — – —, wall – – –.

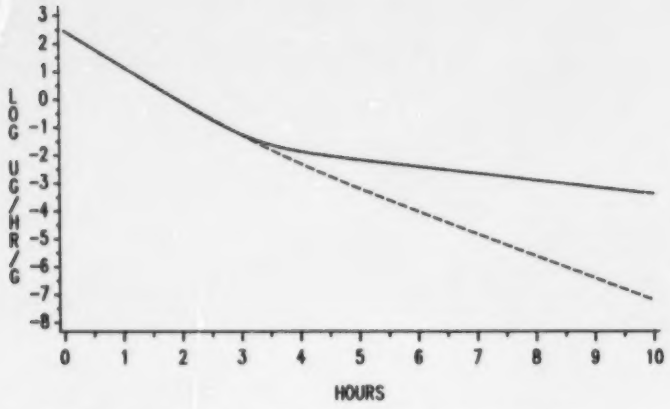

Fig. 6. Butyl propionate emission rate for latex caulk at 23°C, 50% r.h., and 1.85 ACH. ER ——, ER ($k_3 = 0$) - - -.

factor (ERF) are given precise definitions as a result. Rather trivially, the effect of a chamber sink is adjusted out simply by setting to zero the rate constant which governs sink adsorption–absorption. On a more ambitious scale, these results provide a mathematical framework in which the sink constants for the test chamber can be replaced by those of an actual living–working environment, the concentration in that environment then being estimated from the appropriate model. Clearly, this can answer "what if" questions concerning untested combinations of sources and sinks. It also adds motivation to the use of controlled test chambers in order to ascertain the sink properties of various indoor building materials.

Acknowledgement—This research was accomplished with partial support from the U.S. Environmental Protection Agency under Contract No. CR-812305-01-0.

REFERENCES

Dunn J. E. (1987) Models and statistical methods for gaseous emission testing of finite sources in well-mixed chambers. *Atmospheric Environment* 21(2), 425–430.

Godish T. and Rouch J. (1985) An assessment of the Berge equation applied to formaldehyde measurements under controlled conditions of temperature and humidity in a mobile home. *J. Air Pollut. Control Ass.* 35(11), 1186–1187.

Nelms L. H., Mason M. A. and Tichenor B. A. (1987) Determination of emission rates and concentration levels of *p*-dichlorobenzene from moth repellent. *Proc. 80th Ann. Mtg Air Poll. Control Ass.*, paper no. 87–83.6.

Renes S., Leaderer, B. P., Schaap L., Verstraelen H. and Tosun T. (1985) An evaluation of sink terms in removing NO_2 and SO_2 from indoor air. *CLIMA* 2000 4, 221–226.

Sanchez D. C., Mason M. A. and Norris C. L. (1987) Methods and results of characterization of organic emissions from indoor materials. *Atmospheric Environment* 21 (2), 337–345.

SAS Institute, Inc. (1985) *SAS User's Guide: Statistics*, Version 5. Cary, NC.

Seifert B. and Schmahl H. (1987) Quantification of sorption effects for selected organic substances present in indoor air. *Proc. Indoor Air* '87, Vol. 1, pp. 252–256.

NOTICE

This document has been reviewed in accordance with U.S. Environmental Protection Agency policy and approved for publication. Mention of trade names or commercial products does not constitute endorsement or recommendation for use.

This article documents research that was conducted under the auspices of the U.S. Environmental Protection Agency (USEPA). As an arm of the government, the USEPA has a paid up, non-exclusive, irrevocable, worldwide license to reproduce, prepare derivative works, and distribute to the public all of the material contained herein, and to grant others acting on its behalf the right to do so. The USEPA grants to the National Technical Information Service, Department of Commerce, the right to act as its agent in the distribution of this material.